Control of Grid Integrated PV Based Microgrid for Seamless Operation

Burak Onar*,**‡, Sevki Demirbas***

*Electronic and Automastion Dep. Başkent University Anadolu OSB Vocational School, 06909 Malıköy/Ankara/Turkey
**Graduate School of Natural and Applied Sciences, Gazi University, 06500 Beşevler/Ankara/Turkey
***Electric and Elektronic Engineering, Faculty of Technology, Gazi University, 06500 Beşevler/Ankara/Turkey
(burakonar@baskent.edu.tr, demirbas@gazi.edu.tr)

‡Corresponding Author; Burak Onar, Başkent University Anadolu OSB Vocational School, 06909 Ankara, Turkey, Tel: +90 537 216 5470, burakonar@baskent.edu.tr

Received: 28.02.2025 Accepted:27.03.2025

Abstract- In this paper, a controller design has been implemented for PV based Microgrid (PVMG) connected to the grid. The PV system under consideration is linked to the DC bus via a boost converter in order to obtain maximum power, and the DC line is tied up to the AC line, interconnected to the grid through the PCC while supplying the loads, over an inverter. It has also been operating in either island or grid-integrated mode. Although converter topologies remain unchanged across operating modes, the control structures must be adapted accordingly. Additionally, fast and reliable control architecture should be realized to ensure a seamless transition between operating modes. To achieve constant DC with maximum power from the PV, the Perturb&Observe (P&O) algorithm has been used. To convert DC power to AC, the inverter has been controlled with PI based control algorithm. Proposed control structures have been verified based on the simulation performed under Matlab/Simulink.

Keywords Microgrid; smartgrid; seamless transition; PV; grid integrated.

1. Introduction

The need to reduce fossil fuel dependence, address environmental concerns, and mitigate climate change has accelerated the adoption of renewable energy sources (RES) worldwide. The global cumulative installed renewable energy capacity reached 3.9 TW in 2023 [1], and the goal of tripling global capacity by 2030 is what governments set at the COP28 climate change conference organized in Dubai in December 2023 [2].

Although several renewable sources, such as wind, solar, biomass, and hydrogen, have been used for generating power, photovoltaic energy is one of the most important renewable energy sources among these due to its large amount of availability, ease of reach, environmentally friendly, ease of installation, and less maintenance [3]. It has been determined that a grid-connected PV system, when integrated into a fuel station, can meet the energy demands and generate approximately 85,250 kilowatt-hours of energy annually [4]. This has significantly contributed to the reduction of CO_2 emissions each year. The system can allocate approximately 13% of the generated energy for EV charging and around 25% for operating other essential equipment. The investment costs are expected to be recovered within six years. One of the main challenges of PV systems, which are among the renewable energy sources, is the condition of partial shading [5]. This clouding effect has shown its impact on the power-voltage (P-V) curve of a PV array by causing multiple local maximum power points. Consequently, to extract the maximum power under varying conditions caused by shading, commonly used methods such as Perturb and Observe (P&O) and Incremental Conductance (IC) have been employed. Since the performance and efficiency of the PV, however, depend on environmental conditions such as temperature, dust distribution, soiling, shade, and irradiance, it is difficult to predict generated power and to ensure power stability. The inherently intermittent and stochastic structure of PV also affects the integrated power system stability. Additionally, in the event that PV is set up as a grid-connected microgrid, a fast, reliable connection should be equipment between the microgrid and utility grid to establish a smooth transition between islanded and grid-connected modes. PVs are usually connected to the grid via an inverter to secure smooth transition between the modes. Under regular grid-connected mode operation, the inverter supplies maximum power to the

grid with the help of auxiliary services and operates in the current control mode. In islanded mode, PV disconnects from the grid, and power converters operate grid forming voltage controlled mode to establish voltage and frequency stability for loads. As the installation of solar photovoltaic (PV) systems increases, there is a growing need for new studies to monitor and optimize the maintenance management of PVs [6]. In this context, control topologies and studies focused on data collection during both fog and cloud periods have implemented a holistic model for monitoring, maintenance, and management of PVs, considering the Internet of Things (IoT).

In the literature, several control structures have been proposed to guarantee seamless transitions between the operating modes. A state tracking control has been introduced in [7] to pass from grid-connected to not grid-connected mode with stably. In order to ensure a smooth transition in grid-connected systems, state monitoring control is applied between power control and voltage control to provide a smooth transition to the islanding mode. By using residential local DGs, reactive power demand, harmonic currents, and load unbalance have been adapted with power control modification [8]. An adaptive control method has been proposed in [9] for grid-connected conventional power sharing to overcome problems such as harmonic reduction, DC-line voltage regulation rapidly, and uniform transitions between operating modes for the power system in a grid-connected PV system with a battery storage unit. A simple voltage control has been used for the islanding mode of a hybrid microgrid system in which PV and battery energy storage systems (BESS) exist [10]. With the help of a voltage band technique, the switching between charging and discharging modes has been eliminated. The power system, consisting of PV panels and a battery energy storage system, presents the design of a battery charging circuit operating with a maximum power point tracking (MPPT) algorithm using the perturb and observe (P&O) method [11]. The goal is to improve the efficiency of the system by operating the PV system under variable environmental conditions, reduce costs, minimize battery losses, improve its condition, and extend its lifespan. In a microgrid system with a grid-connected PV and battery energy storage system (BESS), active power is transitioned with the grid to improve grid current dynamics and power balance for critical load applications [12]. With increasing concerns over carbon emissions, energy crisis, and power quality, distributed energy resources have much attention [13]. In addition, a variable digital filter (VDF) is used to achieve decision-making capability through distributed control in terms of bidirectional power flow. A single-phase PV with battery energy storage (BES) based hybrid system is used for uninterruptible transmission and power quality (PQ) improvement [14]. In grid-connected mode, current control is used with a learning quantization (LQ) based PV feed-forward (PVFF) loop. The effectiveness of LQ-based current control for load voltage control in islanding mode operation. The impact of reverse power flow on voltage stability is crucial. In this context, reducing reactive power output from photovoltaic (PV) inverters connected to distribution grids has become a priority [15]. It has been determined that the effect of uncertain factors on reducing reverse reactive power increases as PV capacity levels rise. Additionally, it has been observed that the value of power factor adjustment reduces reactive power in the PV grid-connected section. Fixed frequency third-order generalized integrator (AFFTOGI) controller is used to estimate the load fundamental and quadrature components from the distorted grid and unbalanced load [16]. Some types of renewable energy prioritize the use of DC voltage, making the DC voltage grid an essential part of the power system [17]. The performance of a grid-connected PV system with DC voltage has been examined against environmental impacts. To improve the system's performance, a DC-DC converter with an MPPT algorithm and PI controller has been used to provide maximum power to the DC grid. In addition, a fast detection system is presented to switch the DC microgrid to islanding mode, which offers a seamless exchange between an interconnector and a DC microgrid [18]. The grid-connected PV system based on a multilevel-cascaded inverter (MCI) consists of a conventional three-phase VSI and the main grid [19]. The output voltage levels will be maximized by using the asymmetry between the DC voltages of the single-phase and three-phase bridge inverters. A control strategy for this three-phase MCI, based on sliding mode and proportional-integral (PI) linear controllers, has been applied to obtain the SPWM modulator parameters. PI regulator is used to achieve uninterrupted interconnection between the PV-based microgrid and the utility grid. In general, a PI-based simple control strategy is used for smooth switching in a microgrid system with PV-distributed generation [20]. In islanding mode, the PI control regulates the voltage while controlling the current in grid connection mode. Model predictive control (MPC) is proposed for a grid-connected voltage-source inverter to guarantee seamless transfer between grid-connected and islanding modes [21, 22]. When PI-based control and MPC are compared, MPC is implemented simply by adjusting a single parameter through the weighting factor. Uninterruptible power transfer using a multi-latency block frequency domain adaptive filter (MDF) for grid-connected solar photovoltaic (PV) is analyzed, and the use of an efficient control that allows uninterruptible transfer between grid-connected and disconnected modes is analyzed in accordance with the IEEE-519 standard [23]. The autonomous control strategy for a smooth transition between operation modes of the microgrid provides smooth state transition within a single control structure, which allows mode switching independent control, while optimal control parameters are investigated to minimize the voltage deviation in the microgrid [24]. Grid-connected PV microgrid systems have been addressed with ride-through control techniques to minimize potential PV failures and ensure continuity [25]. This approach enhances the microgrid's security and its ability to support the grid. A self-adaptive control strategy has been proposed for a seamless transition between grid and non-grid operations [26]. Using a single drop loop, a robust droop current controller has been implemented and applied to the single-stage inverters fed from PV [27]. By tracking the current, a seamless switching control strategy is proposed [28]. Some intelligent control techniques have also been applied for seamless transitions [29, 30]. By using a machine learning algorithm and a hybrid control strategy, a transition control approach has been developed for grid condition monitoring [31]. A classification

of control methods used for the grid-connected PVMG is presented in Table 1

Table 1. Comparison of control methods used for grid-connected PVMG

Control Methods Used in the Literature	Advantage	Disadvantages
Model Predictive Control (MPC) [21,22]	It is used to optimize transitions in multi-mode systems. It can predict future dynamics. It is used to ensure seamless transition in grid-connected microgrids. It is preferred by adjusting a parameter through the adjustment of a weight factor.	The computational costs are high. It requires powerful processors for real-time applications.
Proportional-Integral (PI) Control [18,20]	It is simple and easy to implement. It is sufficiently effective for most systems. It can be easily used in both grid-connected systems and islanded mode systems. It can be used in voltage and current control applications that are cascaded to each other.	Its performance is limited in complex systems. Different methods are used for tuning the PI parameters.
Artificial Intelligence-Based Control (Neural Networks, Fuzzy Logic, Deep Learning) [32]	It has adaptive and learning capabilities. It can perform self-optimization. It can demonstrate superior performance in complex dynamic systems.	Training can take time. The computational cost is high. It may require large data sets.
A state Tracking Control [7]	By monitoring power and voltage control states, it can suppress DC bus fluctuations in islanded mode.	In unplanned islanding, additional control techniques may be required to achieve a smooth transition.
Adaptive Control Method [9]	In addition to stable performance, it facilitates faster convergence and performs global power tracking even under partially shaded conditions. Harmonic reduction DC-line voltage regulation rapidly	Higher performance can be achieved for real-time applications.
Variable Digital Filter (VDF) [13]	Used to achieve decision-making capability through distributed control in terms of bidirectional power flow Improves power quality Harmonic reduction	It has been validated under weak grid conditions.
Fixed Frequency Third-Order Generalized Integrator (AFFTOGI) [16]	Used to estimate the load fundamental and quadrature components from the distorted grid and unbalanced load It improves the microgrid performance.	It is effective in the adjustment of low-order harmonics.
A self-adaptive control [26]	It enables distributed generation sources within the microgrid to respond quickly to local load demands. It provides island mode detection to ensure a smooth voltage profile.	It is supported by the basic control method, PI control, during the reconnection phase.

This paper introduces a control strategy for grid-connected PVMG, to establish a seamless transition between grid and non-grid operations. The PV has been connected to the grid via a DC/DC converter with boosting capability and DC/AC inverter. Three controllers have been employed to control DC/DC converter and inverter to shape power depending on either grid requirements at the grid connected mode or load needs at the islanding mode. One of the controllers controls the DC/DC converter based on operating mode. In case PV operates grid-connected mode, the controller tracks the maximum power with the MPPT algorithm to obtain maximum power from the sun. Otherwise, it acts as a limiter to protect the DC bus from excessive power generated by PV. Two controllers have been engaged for the inverter to shape power based on the requirements of either loads or grid. This paper is organized as follows: Section two introduces PVMG system and control methods, section three gives the simulation results obtained from proposed system and finally the study has been concluded at section four.

2. PV Based Microgrid Architecture

The general architecture of the grid-integrated PVMG without storage is depicted in Fig.1. The main components of the microgrid are PV modules, DC/DC converter, DC/AC inverter, and local loads. The DC power obtained from the PV feeds the DC bus through a DC-DC converter. The DC power at the DC link is converted to the AC with the help of an inverter either to feed AC local loads or to interconnect to the grid. The point of common coupling (PCC), the station equipment with the switchgear and protective devices, is used for feeding AC local loads and serves as an interconnection point between the microgrid and the main grid.

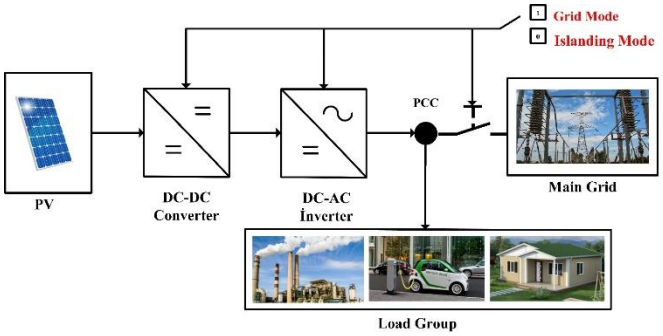

Fig. 1. Simplified block diagram of PVMG.

The PV module is a device combination of PV cells, produced from semiconductor materials and can be described as a current source. PV produces DC power based on certain parameters such as irradiance and environment temperature and its output is characterized by current, voltage, and power. Output characteristics of PV used in this study are given in Fig. 2.

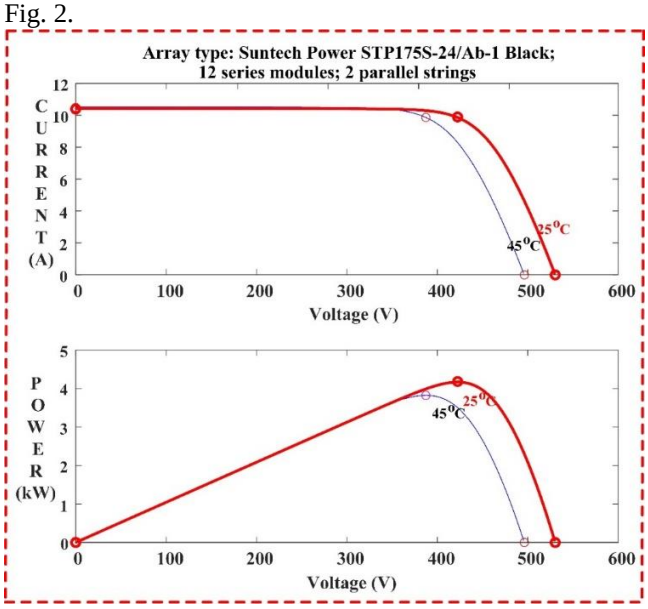

Fig. 2. Output characteristics of PV.

PV and loads need proper DC/DC converter for effective operation. DC/DC converter performs some tasks at the PVMG, such as boosting voltage obtained from PV, controlling power, or MPPT. Although several DC/DC converters can be used based on requirements, boost converter is the most common one in the PV applications. The function of the DC/AC inverter used in a microgrid is to convert DC power obtained from DC/DC converter to AC power needed for local loads and the main grid. Both DC/DC converter and inverter operations are controlled based on operation modes, grid-connected or islanding, and loads and/or grid requirements.

3. PV Control of the PV Based Microgrid

The circuit diagram given in Fig. 3 illustrates the PVMG connected to the grid. As seen from the figure, the power generated by the PV module is transferred to the AC bus via a DC-DC converter, DC-AC inverter and LC filter. The DC link between the DC/DC converter and inverter is used to obtain constant and stable DC voltage for inverter input. This line can also be used as a feeder for DC loads and other RES and storage unit connections.

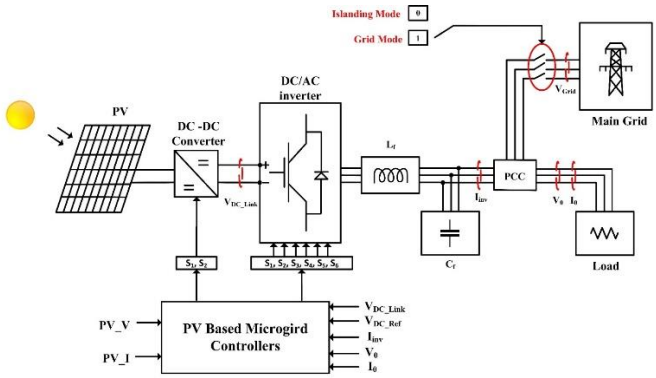

Fig. 3. Circuit diagram of grid-connected PVMG.

DC/DC converter and DC/AC inverter are controlled based on PVMG operation whether it is connected to the grid or not. While the DC/DC converter is used for extracting peak power from PV in grid-connected mode, it regulates the DC link in standalone mode. In this study, the DC voltage obtained from the PV module is boosted through the DC-DC converter to create a DC bus voltage of 800V. The PVMG without storage follows the grid during operation and the inverter is controlled based on the power penetrated to the grid in the grid-connected mode. On the other hand, it is controlled depending on load requirements in the standalone mode.

3.1. Control of DC/DC Converter

The first part of the grid-connected PVMG is the DC-DC converter. Boost converter topology given in Fig. 4 has been used in this study as DC/DC converter. Two different control methods have been used based on operating modes. In order to obtain the maximum power from PV in grid connection mode, PWM switching signal is produced with the duty cycle obtained through the Perturb&Observe (P&O) MPPT algorithm, and V_{DC_Link} voltage is generated. In the islanding mode, the converter is controlled to establish stable DC link voltage. DC link voltage has been regulated with a PI-based control algorithm. As seen in Fig. 4, the DC link voltage is compared with a reference voltage, and a voltage error is achieved. After regulating voltage error with PI controller, a control signal for PWM is generated. The PWM generator converts the control signal to a switching signal to drive the power electronic switch such as IGBT.

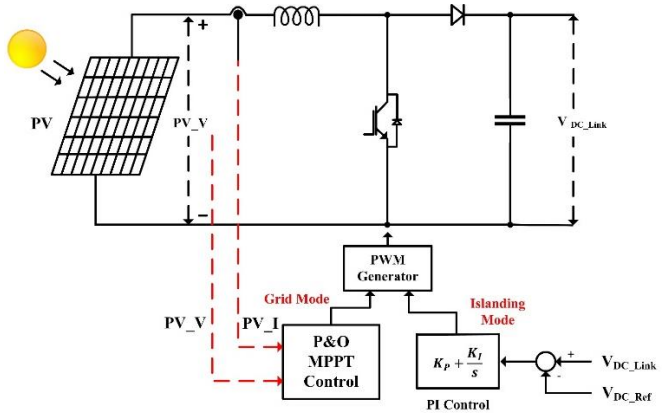

Fig. 4. Circuit diagram of DC/DC converter.

3.2. Control of DC/AC Inverter

DC-AC inverter is the second part of the grid-connected PVMG. It converts DC power to desired AC power for grid or load. Three phase full bridge voltage source inverter (VSI) has been used to convert DC to AC as seen Fig. 5. The VSI is followed by LC filter for harmonics reduction and PCC point with grid connection. The VSI is controlled depending on PVMG operating mode. If PVMG operates grid-connected mode VSI is controlled to supply PV power to the grid. For this purpose, DC link voltage is compared with DC voltage reference and current references at *dq* frame is achieved. Later, *dq* reference currents are compared with the *dq* currents received from the transform measured *abc* current to *dq* current.

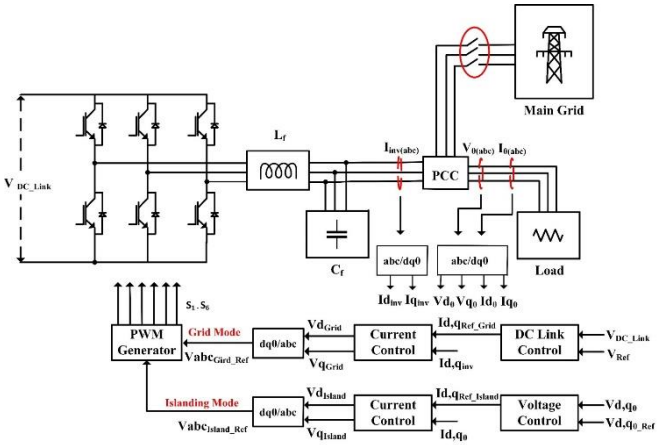

Fig. 5. Circuit diagram of DC/AC inverter.

The current control method shown in Fig. 6. and Eq. (1,2) is applied to *dq* currents, and then *dq* voltage references are obtained. After the *dq/abc* voltage transform, *abc* voltage references used for PWM generation are produced. Carrier-based PWM technique is used for picking up switching signals for IGBTs using a PWM generation block.

$$e_{I_{Grid_{d,q}}} = I_{d,q_{ref}} Grid - I_{d,q_{inv}} \quad (1)$$

$$V_{d,q_{ref_{Grid}}} = K_p e_{I_{Grid_{d,q}}}(t) + K_i \int_0^t e_{I_{Grid_{d,q}}}(\tau)d\tau \pm I_{d,q_{inv}} * \omega L \quad (2)$$

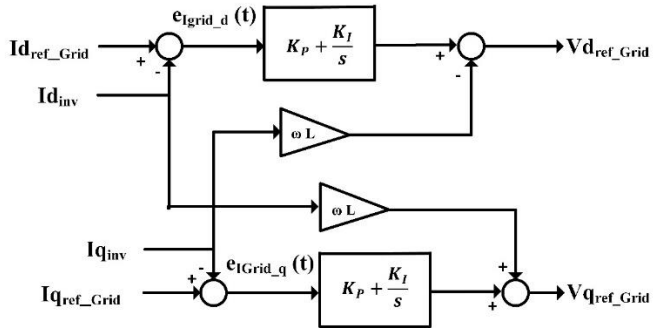

Fig. 6. Current control block diagram for grid connected mode of grid-connected PVMG.

A key challenge in PVMG operation is ensuring a seamless transition between grid-connected and islanding modes. In case PVMG moves from grid-connected mode to islanding mode, planned or not planned, PVMG must restore grid stability and must continue to supply loads. VSI forms the MG based on given ideal reference voltages and fixed frequency in the standalone mode. In this study *dq* axis reference voltages have been set to 220√2 V, and zero respectively, and a two-stage controller is applied to the VSI.

The first stage is voltage controller, where current references in *dq* frame is produced from given reference voltages as given in Fig. 7. In this control, reference voltages in *dq* frame are compared with *dq* voltages obtained from *abc/dq* transform of measured voltages at the load side. After regulating voltage differences with PI control, and decoupled with ωC references in *dq* frame obtained. Eq. (3,4) define the expression used for retrieving *dq* reference currents.

$$e_{U_{d,q_0}} = V_{d,q_0} - V_{d,q_{0_{ref}}} \quad (3)$$

$$I_{d,q_{ref_{Island}}} = K_p e_{U_{d,q_0}}(t) + K_i \int_0^t e_{U_{d,q_0}}(\tau)d\tau \pm V_{d,q_0} * \omega C \quad (4)$$

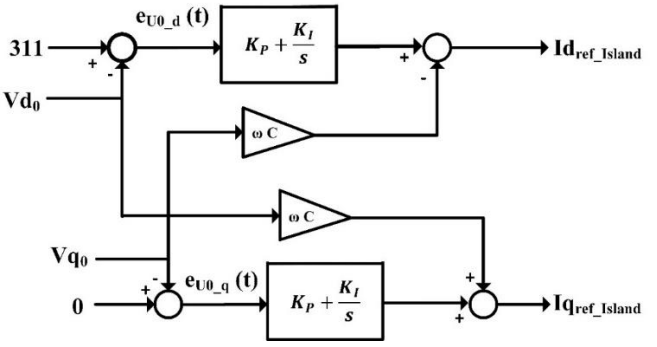

Fig. 7. Voltage control block diagram for islanding mode of grid-connected PVMG.

The second stage of inverter control in islanding mode is current control illustrated in Fig. 8. In this step, *dq* reference currents calculated at Eq. (4) are compared with the *dq* currents achieved from measured *abc* currents to *dq* conversion and current differences between reference and actual current in *dq* frame received as indicated in Eq (5). As defined in Eq. (6), current differences in *dq* frame regulated

with PI control and *dq* voltage references produced after decoupling with ωL. Eventually, *abc* reference voltages for PWM generator is performed with *dq/abc* conversion. PWM generation block generate switching signals for IGBTs by using carrier-based PWM technique.

$$e_{I_{d,q_{inv}}} = I_{d,q_{ref_{Island}}} - I_{d,q_{inv}} \quad (5)$$

$$V_{d,q_{ref_{Island}}} = K_p e_{I_{d,q}}(t) + K_i \int_0^t e_{I_{d,q}}(\tau)d\tau \pm I_{inv_{d,q}} * \omega L \quad (6)$$

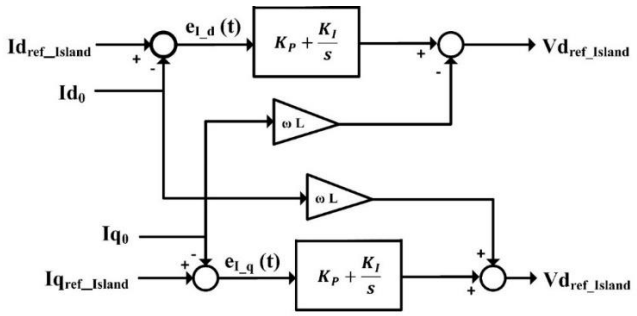

Fig. 8. Current control block diagram for islanding mode of grid-connected PVMG.

3.3. Control of angular velocity in PVMG

The frequency stability is another important point that must fulfill load and grid requirements. The frequency stability is ensured by DC/AC inverter. The PLL block diagram given in Fig. 9 is used for providing frequency and angular velocity data at the output depending on the voltage data given at the input.

In grid-connected mode reference frequency is provided by main grid. Therefore, with the V_{Grid} voltage value received from the grid in the grid-connected PVMG system, ωt_{Grid} data is used in all control blocks and is obtained at the output. However, when the microgrid system is disconnected from the grid and transitions to island mode since there is no voltage data to be taken as a reference, inner voltage references are needed. 3-phase voltage data V_{Ref} with a phase difference of 120^0 degrees and 50 Hz frequency is used as an inner reference voltage, and ωt_{Island} angular position data is obtained.

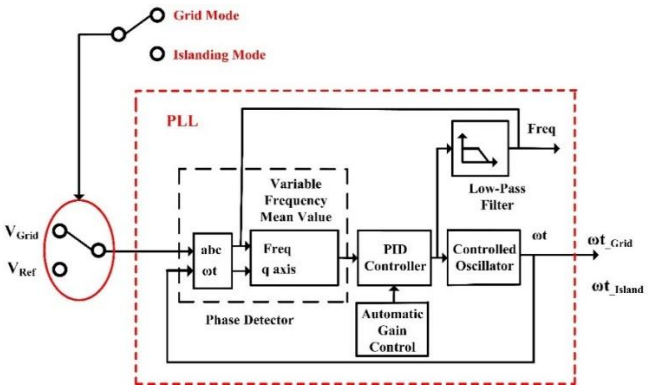

Fig. 9. Control block diagram of grid-connected PVMG.

4. Simulation Result

The presented control scheme is applied to the PVMG given in Fig. 3 and performance has been simulated at different conditions. to a smooth transition between the operating modes and validated with simulation. The PV source used for simulation is a 4.2 kW PV module whose output characteristics are given in Fig. 2. 800 V DC bus voltage and 1 kW local loads have been preferred in the simulation. The sampling time of the simulation has been chosen as 10 μs, and a 10 kHz switching frequency has been selected for both DC/DC converter and DC/AC inverter. The PI parameters have been tuned based on traditional methods such as trial and error methods. The simulation was performed for 2 seconds under different operating conditions. Once the PVMG has been simulated under grid-connected mode until 0.5 seconds, then switched to the islanding mode at 0.5 seconds and continued to operate until 1. second, it has been switched to grid connected mode again and has been kept for 0.5 seconds in this mode. Finally, the PVMG moved from grid connected mode to islanding mode at 1.5 seconds and ran the end of the simulation. Results obtained from the simulation have been summarized in Fig. 10-21.

One of the controlled parameters in this study is DC link voltage. DC/DC converter has been employed to convert PV power to constant DC power. It has been controlled based on the operating mode, and DC link voltage should be stable during the transient between the operating modes. As seen in Fig. 10, the DC link voltage suddenly increases to 858 V for a short time and settles to 800 V in 0.07 seconds. During the transition times between the operating modes, small DC voltage transients (about 4 V) occur for a very short time (about 0.03 seconds). In other words, a 0.5% voltage spike has ensured stability for a duration of 1.5 cycles (0.03 seconds).

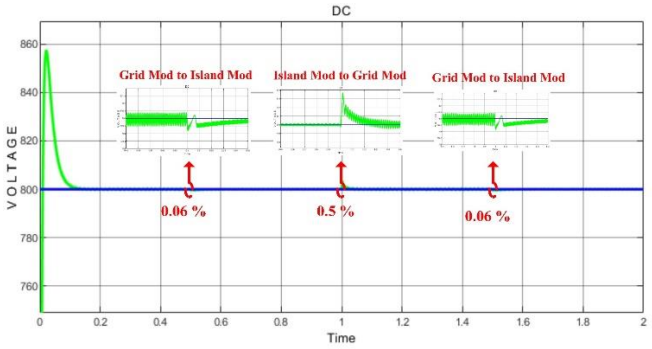

Fig. 10. DC bus stability graph of grid-connected PVMG.

Fig. 11-13 shows the voltage and current waveforms under the transient from grid-connected mode to islanding mode. The voltage and current waveforms obtained from LC filter output and grid side measurement are given in Fig. 11 and Fig. 12 respectively. It can be observed from the figures that, while voltages are not affected by transient currents disturbances restored less than half cycle. In addition, it is observed that no significant voltage fluctuations and current harmonics occur during the transition to island mode. Thus, a smooth transition was ensured. Fig. 13 shows the voltage and current measurements taken from the PCC point. As seen from the figure voltages and currents remain stable under transient.

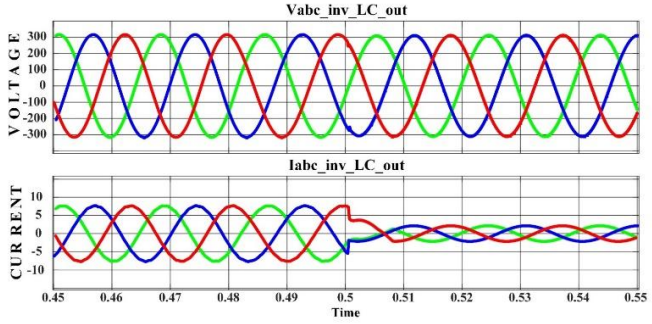

Fig. 11. Moment of transition of grid-connected PVMG to island mode in 0.5 seconds (measurement taken from inverter LC Filter output).

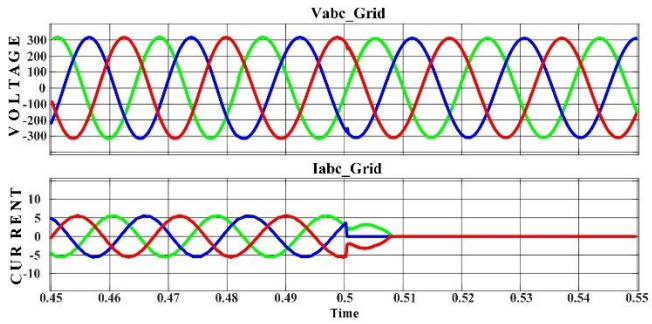

Fig. 12. Moment of islanding of grid-connected PVMG at 0.5 seconds (grid-side measurement).

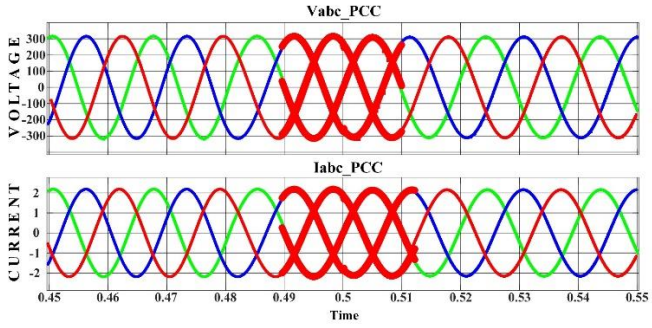

Fig. 13. Moment of islanding of grid-connected PVMG at 0.5 seconds (measurement from PCC point).

Voltage and current waveforms during transient from islanding mode to grid connected mode are given in Fig. 14 – 16. Fig. 14 and Fig. 15 show the voltages and current waveforms at the output of the LC filter and grid side. It can be seen from the figures voltages remain stable all the time by means of amplitude and frequency. In Fig. 14 local loads draw 2 A current from the PVMG before switching grid connected mode and power produced from PV is limited in this mode. After 1. second, PVMG connected to the grid again, and maximum power was drawn from the PV, and 5 A current penetrates the main grid. Because PVMG is not connected to the grid before 1. second measured current seems zero in Fig. 15. Fig. 16 illustrates the voltage and current waveforms taken from the PCC point. As seen from the figure voltages and currents remain stable under transient.

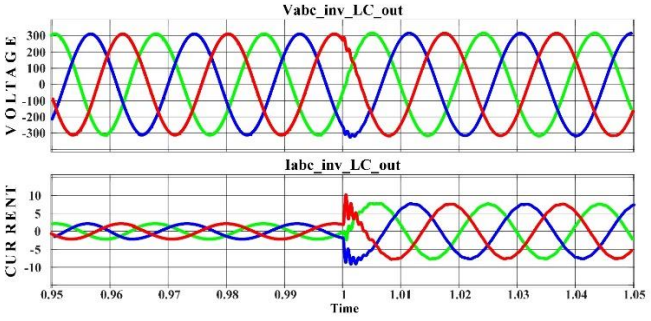

Fig. 14. The moment when grid-connected PVMG transition to grid connection mode in the 1st second (inverter LC filter output measurements).

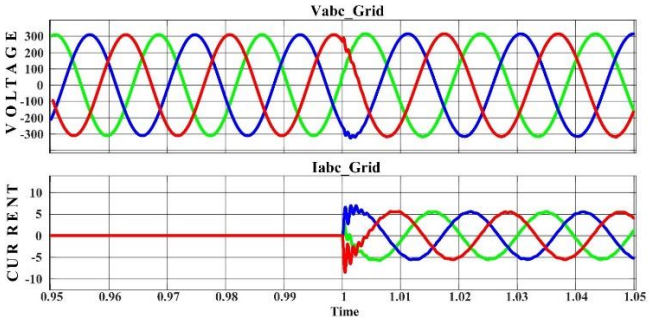

Fig 15. The moment when grid-connected the PVMG transitions to grid connection mode in the 1st second (measurements taken from the grid side).

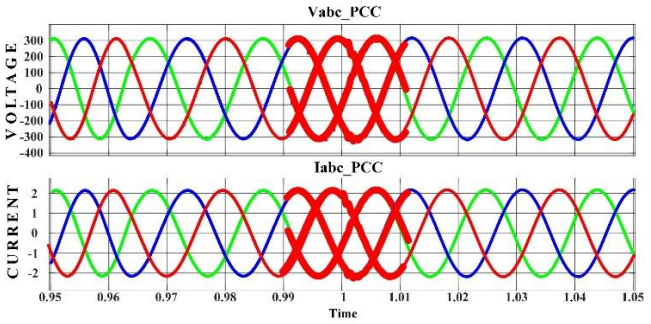

Fig. 16. The moment when grid-connected the PVMG transition to grid connection mode in the 1st second (measurements from PCC point).

The grid-connected PVMG was operated under a 1 kW load throughout the entire simulation for both grid-connected mode and island mode. The results of load increase and decrease scenarios for both operating modes were analyzed at the PCC point. In this context, when the load supplied by the PVMG operating in grid-connected mode was increased from 1 kW to 2 kW at 0.15 seconds, as shown in Fig. 17, the load was then reduced back to 1 kW at 0.25 seconds, ensuring continuous operation under a 1 kW load. When the grid-connected PVMG transitioned to island mode, its operation under different loads was monitored, and a seamless transition was achieved. In this regard, as illustrated in Fig. 18, the PVMG operating in island mode underwent a load increase from 1 kW to 2 kW at 0.66 seconds, followed by a load reduction at 0.77 seconds, maintaining operation under a 1 kW load. The smooth transitions of the PVMG under different load conditions in island mode confirm its stable operation.

Thus, the response of the grid-connected PVMG to sudden transitions under different loads in both operating modes demonstrates that a seamless transition has been achieved.

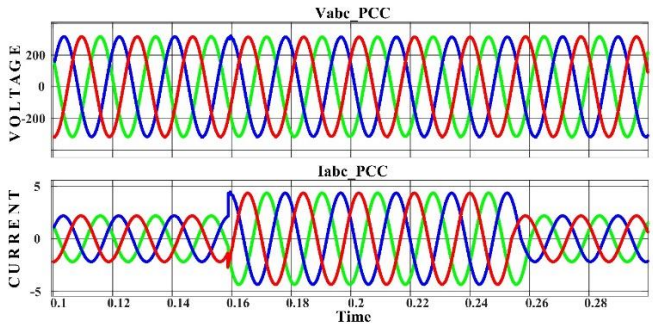

Fig. 17. Sudden load change during the operation of the grid-connected PVMG in grid-connected mode (measurements from PCC point).

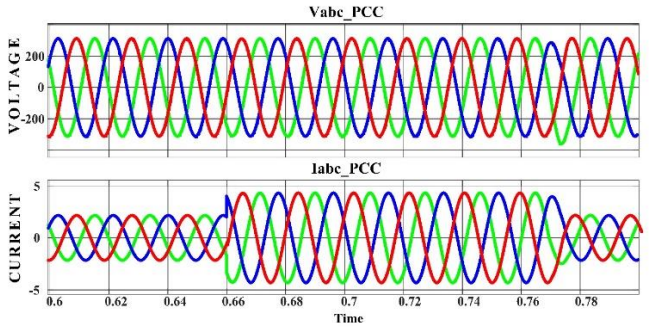

Fig. 18. Sudden load change during the operation of the grid-connected PVMG in island mode (measurements from PCC point).

Although remarkable changes do not occur during the transition between the modes, it is necessary to analyze harmonic distortion. Therefore, the harmonic distortion that occurs during the transitions between the operating modes at 0.5, 1 and 1.5 seconds is clearly indicated in the THD graph in Fig. 19. According to the IEEE-519 standard, the THD ratio in grid connected systems is required to be below 5%.

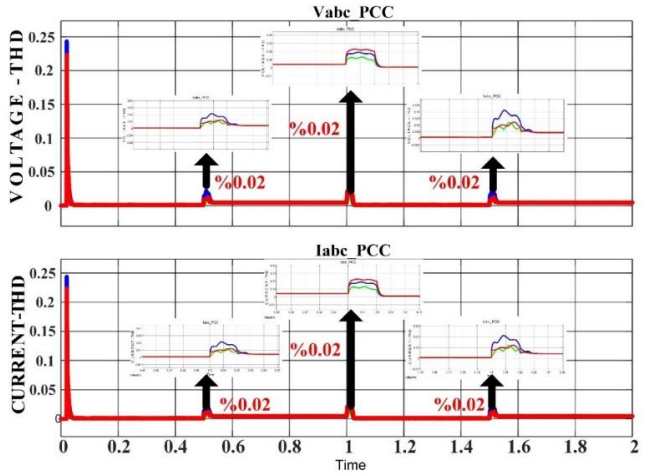

Fig. 19. THD graph at the moments of transition between operating modes during the simulation period (measurements taken at the inverter LC filter output).

In this study, it is proved that the inverter LC filter output graph given in Fig. 19 is well below this ratio. In addition, the fact that the harmonic distortion rate is below 3% according to the THD graph of the current-voltage graphs taken from the PCC point given in Fig. 20, which shows the moments of switching between operating modes at 0.5, 1 and 1.5 seconds, is an indication that the grid-connected PVMG we designed has a smooth transition between operating modes.

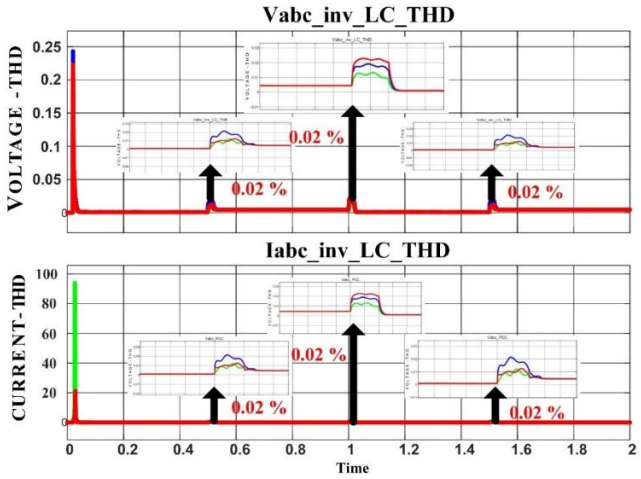

Fig. 20. THD graph at the moments of transition between operating modes during the simulation period (measurements taken at point of PCC).

5. Conclusion

In the proposed study, the findings obtained from simulation results verify that the transitions between the operating modes of the grid-connected microgrid are carried out smoothly. Although the grid-connected PVMG is structurally a highly complex system, it has been reliably controlled using a PI-based control method, which offers simple, safe, and fast solutions. According to the obtained results, the voltage and current transients occurring during mode transitions comply with the IEEE-519 standard. Consequently, the PVMG has maintained uninterrupted operation and stability during transitions between operating modes. The contributions of the proposed controller to the literature are as follows: i) ensuring DC bus voltage stability, ii) enabling smooth transitions between operating modes by maintaining stability at the PCC, and iii) preserving the stability of the PVMG under load increase or decrease conditions. These have been verified through the obtained findings. The proposed study has been validated through simulation studies conducted in the Matlab & Simulink environment. In addition, it is considered that integrating a battery energy storage system into the proposed system would further contribute to the stability of the PVMG.

Acknowledgments
This study was made possible by FGA-2023-9043 from the Gazi Universty Coordinatorship of Scientific Research Projects. The statements made herein are solely the responsibility of the authors.

References

[1] Global Renewable Power Capacity 2023 | statista, https://www.statista.com/statistics/1094331/global-renewable-capacity-cumulative/ (accessed Apr. 5, 2025).

[2] Iea, "Executive summary – COP28 tripling renewable capacity pledge – analysis," IEA, https://www.iea.org/reports/cop28-tripling-renewable-capacity-pledge/executive-summary (accessed Apr. 5, 2025).

[3] A. A. Mahmoud, A. A. Hafez, A. M. Yousef, M. A. Gaafar, Mohamed Orabi and A. F. M. Ali, "Fault-tolerant modular multilevel converter for a seamless transition between stand-alone and grid-connected microgrid," IET Power Electronics, vol. 16, no. 1, pp. 11–25, Jul. 2022. doi:10.1049/pel2.12359.

[4] F. A. Aljohani, A. Z. Alabideen, M. E. Tero, B. A. I. Alamrety, N. S. Alharbi, M. M. Alrehaili and A. I. Alkassem, "On-grid PV-EV charging station system," 2024 12th International Conference on Smart Grid (icSmartGrid), pp. 355–361, May 2024. doi:10.1109/icsmartgrid61824.2024.10578294.

[5] S. Hadji, L. Larbi, A. Belkaid, I. Colak, and R. Bayindir, "Global Optimum Operating Point Tracker of PV system, under partial shading, using parallel searching," 2022 10th International Conference on Smart Grid (icSmartGrid), pp. 227–230, Jun. 2022. doi:10.1109/icsmartgrid55722.2022.9848552.

[6] M. K. Amaehule, R. Uhunmwangho, N. Nwazor and K. E. Okedu, "Smart intelligent monitoring and maintenance management of photo-voltaic systems," International Journal of Smart grid, vol.6 no. 4, pp. 110-122 dec. 2022. doi:10.20508/ijsmartgrid.v6i4.260.g246.

[7] Z.-W. Qu, Z.-X. Chong, Y.-J. Wang, Z. Shi, and Y.-X. Yao, "Control method for grid-connected/islanding switching of Hybrid AC/DC Microgrid," Journal of Electrical Engineering & Technology, vol. 18, no. 1, pp. 15–25, Jul. 2022. doi:10.1007/s42835-022-01146-8.

[8] G. G. Talapur, H. M. Suryawanshi, L. Xu, and A. B. Shitole, "A reliable microgrid with seamless transition between grid connected and islanded mode for Residential Community With Enhanced Power Quality," IEEE Transactions on Industry Applications, vol. 54, no. 5, pp. 5246–5255, Sep. 2018. doi:10.1109/tia.2018.2808482.

[9] P. K. Sorte, K. P. Panda, and G. Panda, "Current reference control based MPPT and investigation of power management algorithm for grid-tied solar PV-Battery System," IEEE Systems Journal, vol. 16, no. 1, pp. 386–396, Mar. 2022. doi:10.1109/jsyst.2021.3052959.

[10] S. Jain, S. Dhara, and V. Agarwal, "A voltage-zone based power management scheme with seamless power transfer between PV-battery for off-grid stand-alone system," IEEE Transactions on Industry Applications, vol. 57, no. 1, pp. 754–763, Jan. 2021. doi:10.1109/tia.2020.3031265.

[11] L. Larbi, S. Hadji, A. Belkaid, I. Colak, and R. Bayindir, "Design of a buck converter battery charging controller in PV Plant," 2022 10th International Conference on Smart Grid (icSmartGrid), pp. 214–220, Jun. 2022. doi:10.1109/icsmartgrid55722.2022.9848640.

[12] O. P. Jaga and S. GhatakChoudhuri, "A smart control for self-reliant single-phase, grid-tied photovoltaic-battery storage system," Sustainable Energy Technologies and Assessments, vol. 57, p. 103269, Jun. 2023. doi:10.1016/j.seta.2023.103269.

[13] P. Shukl and B. Singh, "Seamless transition of PV-bes microgrids with Power Quality Improvement Capability," 2021 IEEE 4th International Conference on Computing, Power and Communication Technologies (GUCON), Sep. 2021. doi:10.1109/gucon50781.2021.9573989.

[14] S. Kumar and B. Singh, "Seamless operation and control of single-phase hybrid PV-bes utility synchronized system," IEEE Transactions on Industry Applications, vol. 55, no. 2, pp. 1072–1082, Mar. 2019. doi:10.1109/tia.2018.2876640.

[15] S. Akagi, S. Kaburagi, K. Ishibashi, K. Okumura, and R. Maeda, "Evaluation of the impact of uncertainty on reactive power reduction through fixed power factor adjustment of PV systems in medium-voltage distribution networks," 2024 13th International Conference on Renewable Energy Research and Applications (ICRERA), pp. 612–616, Nov. 2024. doi:10.1109/icrera62673.2024.10815182.

[16] V. Kumar, G. Modi, and B. Singh, "AFFTOGI control for power quality improvement and seamless transition in grid-tied SPV-Bes System," 2021 IEEE 4th International Conference on Computing, Power and Communication Technologies (GUCON), Sep. 2021. doi:10.1109/gucon50781.2021.9573914.

[17] E. Kurt and G. Soykan, "Performance analysis of DC Grid Connected PV system under irradiation and temperature variations," 2019 8th International Conference on Renewable Energy Research and Applications (ICRERA), pp. 702–707, Nov. 2019. doi:10.1109/icrera47325.2019.8996577.

[18] V. Kleftakis, D. Lagos, C. Papadimitriou, and N. D. Hatziargyriou, "Seamless transition between interconnected and islanded operation of DC microgrids," IEEE Transactions on Smart Grid, vol. 10, no. 1, pp. 248–256, Jan. 2019. doi:10.1109/tsg.2017.2737595.

[19] V. F. Pires, J. Monteiro, and J. F. Silva, "A grid-connected PV multilevel cascaded inverter system based

on single and three-phase two-level inverters," 2019 8th International Conference on Renewable Energy Research and Applications (ICRERA), pp. 118–123, Nov. 2019. doi:10.1109/icrera47325.2019.8996765.

[20] A. M. Mansour, O. M. Arafa, M. I. Marei, I. Andelsalam, G. A. Aziz and A. A. El-sattar, "Seamless control for a PV system during transitions between grid connection and standalone operation," 2019 21st International Middle East Power Systems Conference (MEPCON), Dec. 2019. doi:10.1109/mepcon47431.2019.9008071.

[21] X. Li, H. Zhang, M. B. Shadmand, and R. S. Balog, "Model predictive control of a voltage-source inverter with seamless transition between islanded and Grid-Connected Operations," IEEE Transactions on Industrial Electronics, vol. 64, no. 10, pp. 7906–7918, Oct. 2017. doi:10.1109/tie.2017.2696459.

[22] X. Li, H. Zhang, and R. Balog, "Control strategy for seamless transfer between Island and grid-connected operation for a dual-mode photovoltaic inverter," 2015 IEEE Energy Conversion Congress and Exposition (ECCE), Sep. 2015. doi:10.1109/ecce.2015.7310499.

[23] B. Singh and P. Shukl, "Seamless power transfer of solar PV based Grid Interactive System," 2021 National Power Electronics Conference (NPEC), Dec. 2021. doi:10.1109/npec52100.2021.9672533.

[24] Y. Li, L. Fu, K. Meng, K. Muttaqi and W. Du, "Autonomous Control Strategy for microgrid operating modes smooth transition," IEEE Access, vol. 8, pp. 142159–142172, 2020. doi:10.1109/access.2020.3014255.

[25] I. E. Davidson and E. Buraimoh, "Modelling of a photovoltaic-based grid supporting microgrid and fault ride-through Control Application," International Journal of Smart grid, vol.7, no.2, pp. 69-83, june 2023. doi:10.20508/ijsmartgrid.v7i2.284.g273.

[26] Y. Singh, B. Singh, and S. Mishra, "Control of single-phase distributed PV-battery microgrid for smooth mode transition with improved power quality," IEEE Transactions on Industry Applications, vol. 58, no. 5, pp. 6286–6296, Sep. 2022. doi:10.1109/tia.2022.3178388.

[27] M. M. Moustafa, M. Aboushal, T. EL-Fouly, A. Al-Durra, and H. Zeineldin, "A novel unified controller for grid-connected and islanded operation of PV-fed single-stage inverter," IEEE Transactions on Sustainable Energy, vol. 12, no. 4, pp. 1960–1973, Oct. 2021. doi:10.1109/tste.2021.3074248.

[28] Q. Xiang, Z. Liao, and T. Li, "A novel control strategy of the seamless transitions between grid-connected and Islanding Operation Modes for the multiple complementary power microgrid," International Journal of Electronics, vol. 108, no. 8, pp. 1381–1400, Feb. 2021. doi:10.1080/00207217.2020.1870726.

[29] M. A. Khan, A. Haque, F. Blaabjerg, V. S. Kurukuru, and H. Wang, "Intelligent transition control between grid-connected and standalone modes of three-phase grid-integrated distributed generation systems," Energies, vol. 14, no. 13, p. 3979, Jul. 2021. doi:10.3390/en14133979.

[30] A. H. EL-Ebiary, M. A. Attia, M. I. Marei, and M. A. Sameh, "An integrated seamless control strategy for distributed generators based on a deep learning artificial neural network," Sustainability, vol. 14, no. 20, p. 13506, Oct. 2022. doi:10.3390/su142013506.

[31] M. A. Khan, A. Haque, and V. S. Kurukuru, "Intelligent transition control approach for different operating modes of photovoltaic inverter," IEEE Transactions on Industry Applications, vol. 58, no. 2, pp. 2332–2340, Mar. 2022. doi:10.1109/tia.2021.3135250.

[32] E. Mohammadi, M. Alizadeh, M. Asgarimoghaddam, X. Wang, and M. G. Simoes, "A review on application of artificial intelligence techniques in microgrids," IEEE Journal of Emerging and Selected Topics in Industrial Electronics, vol. 3, no. 4, pp. 878–890, Oct. 2022. doi:10.1109/jestie.2022.3198504.